

Structure Analysis of a Combined Main-Chain/Side-Group Liquid Crystalline Polymer by Electron Microscopy

I. G. Voigt-Martin*

Institut für Physikalische Chemie der Universität, D-6500 Mainz, West Germany

H. Durst

Max Planck Institut für Polymerforschung, D-6500 Mainz, West Germany

B. Reck and H. Ringsdorf

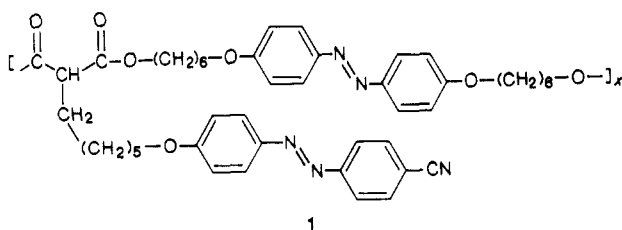
Institut für Organische Chemie der Universität, D-6500 Mainz, West Germany.

Received September 15, 1987

ABSTRACT: The distribution and growth of smectic planes in a combined main-chain/side-group liquid crystal polymer have been demonstrated by dark-field electron microscopy and the orientation of the molecule with respect to the smectic planes has been determined by electron diffraction. In addition, the smectic planes have been imaged by high-resolution electron microscopy. Undulations and defects have been observed.

Introduction

The polymer investigated here is a liquid crystalline main-chain/side-group polymalonate with azobenzene as mesogen in the main chain and cyanoazobenzene as mesogenic side group. Chemical structure, phase transitions, and molecular geometry (from molecular models) of the polymer are indicated in 1 (where the main chain repeating unit length = 35 Å, the side chain length = 24 Å, and the phase transitions (°C) are g 33 k 88 s 195 i).



The polymer belongs to a series of combined polymalonates.¹ This series demonstrates how strongly the mesophase behavior can be influenced by the macromolecular architecture. Most of the polymers exhibit smectic phases above the melting transitions. Small nematic phases can occur¹ only in those cases where there is a large difference between the length of the main-chain and side-group spacer. From the macroscopic properties it has been assumed that the mesogenic side groups arrange themselves parallel to the main-chain mesogens to form a liquid crystalline phase.² Furthermore, the molecular model of the main-chain/side-group polymalonate under investigation suggests that a dense packing of both types of mesogens into a smectic structure is achieved most easily if the main chain is bent and not in the extended chain conformation. This model is demonstrated in Figure 1.

In the following, structural details regarding the smectic phase of this polymer will be elucidated by electron microscopy and electron diffraction.

Experimental Section

Synthesis. The monomers were synthesized as described previously.¹ For the melt polycondensation, a polymer tube charged with 8 g (17.2 mol) of diethyl (6-[(4-((4-cyanophenyl)azo)phenyl)oxy]hexyl)malonate and 7.12 g (17.2 mol) of 4,4'-bis((6-hydroxyhexyl)oxy)azobenzene was flushed with dry nitrogen and heated to 160 °C. The resulting melt was agitated with a magnetic stirrer. Six drops of a mixture of diethylene glycol dimethyl ether and tetraisopropylorthotitanate (volume ratio 9:1) were added to the melt via syringe and rubber septum. After a few minutes, ethanol started to distill. It was removed by a slow

stream of nitrogen passing through the reaction vessel. After 3 h, 5 drops of catalyst solution were added. The temperature was raised to 200 °C, and an aspirator vacuum was applied for 2 h. The polycondensation was completed under high vacuum (<0.1 mbar) for 3 h at 210 °C.

After cooling, the polymer was dissolved in 200 mL of methylene chloride, precipitated twice from 2 L of acetone, and dried in vacuo to yield 13.2 g (98%) of product. Gel permeation chromatography in THF with Styragel 10³/10⁴ columns gave a molecular weight of 64 000 compared to polystyrene standards. The inherent viscosity number determined with a 0.5 wt % solution in chloroform was 0.52 dL/g.

Mesomorphic Properties. The mesophase behavior of the main-chain/side-group polymalonate under discussion was studied by differential scanning calorimetry (DSC) and polarizing microscopy.

The DSC heating curve (Figure 2) reveals a glass transition at 33 °C followed by a recrystallization exotherm and the endothermic melting transition at 88 °C (peak maximum $\Delta H_{k-s} = 3.8$ cal/g). Above the melting temperature, the polymer is in a smectic phase. The transition to the isotropic state occurs at 195 °C (peak maximum $\Delta H_{s-i} = 3.5$ cal/g).

The DSC cooling curve (Figure 2) shows that the smectic phase can be supercooled very easily. Even at a cooling rate of 10 °C/min, the smectic phase can be frozen unchanged into the glassy state. The birefringent texture of the smectic phase was observed between untreated glass slides. Figure 3 shows the typical well-developed striped mosaic texture. This texture is similar to textures documented in the literature for ordered smectic phases like S_B, S_E, or S_H.³

Preparation of Thin Films. The thin films were produced by solution casting as described previously⁴ for a side-group liquid crystal polymer with a 0.1% solution in chloroform. Other solvents such as THF were rejected because of hole formation. By this procedure the films were preoriented but did not give rise to the small-angle diffraction maxima typical of liquid crystals. Orientation was achieved only by subsequently annealing these samples just below the isotropic-smectic transition temperature. Subsequently, the sample was quenched.

Results

Bright-Field Electron Microscopy. The liquid crystal films were deposited on a carbon substrate and shadowed obliquely with Pt/C at an angle of 20°. The replica was subsequently studied by electron microscopy (Figure 4). The film thickness as determined by the shadow length on the carbon substrate was 250 Å. The dark stripes observed in these samples are easier to interpret than those observed in the side-chain polymethacrylate liquid crystal studied previously,⁴ because in contrast to the side-chain system, clear shadows are cast by the oblique shadowing. Therefore, the conclusion is the

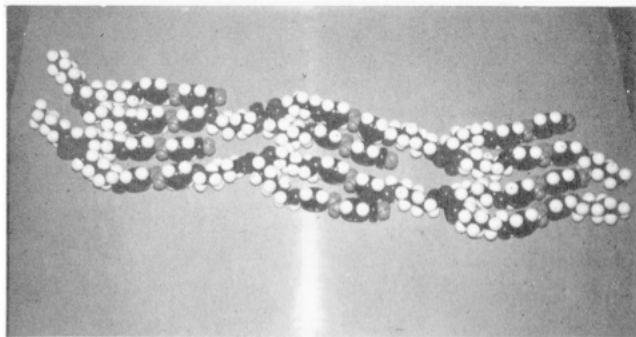


Figure 1. Model showing two polymalonate molecules.

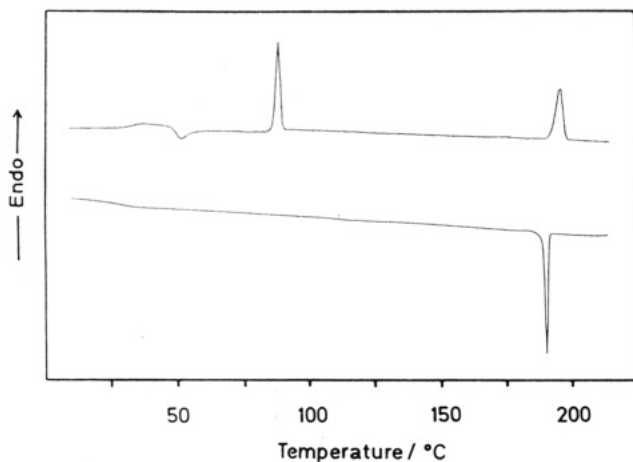


Figure 2. DSC diagram of polymalonate.

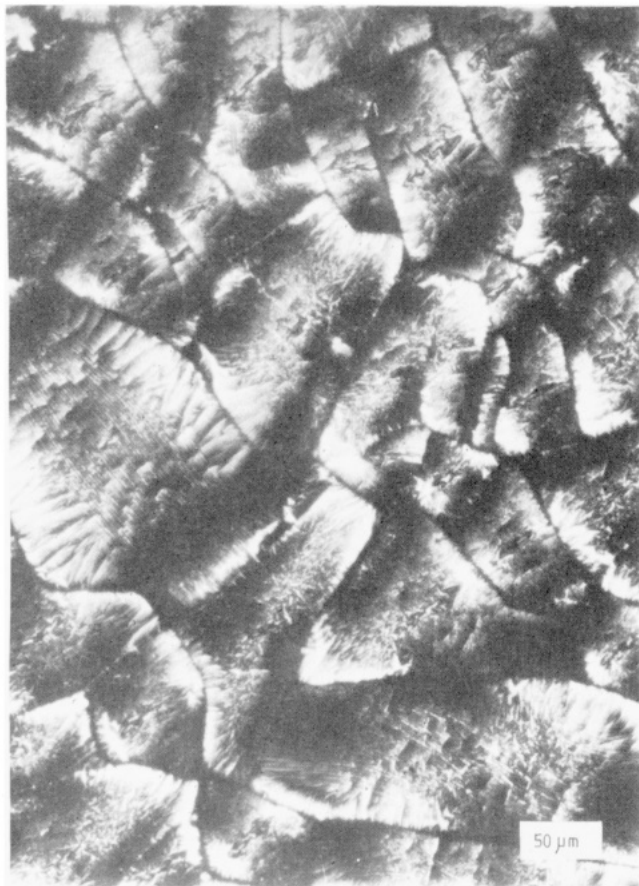


Figure 3. Light micrograph showing main-chain/side-group liquid crystal polymer.

same as that reached previously, namely these dark stripes are caused by scattering contrast due to surface ripple.

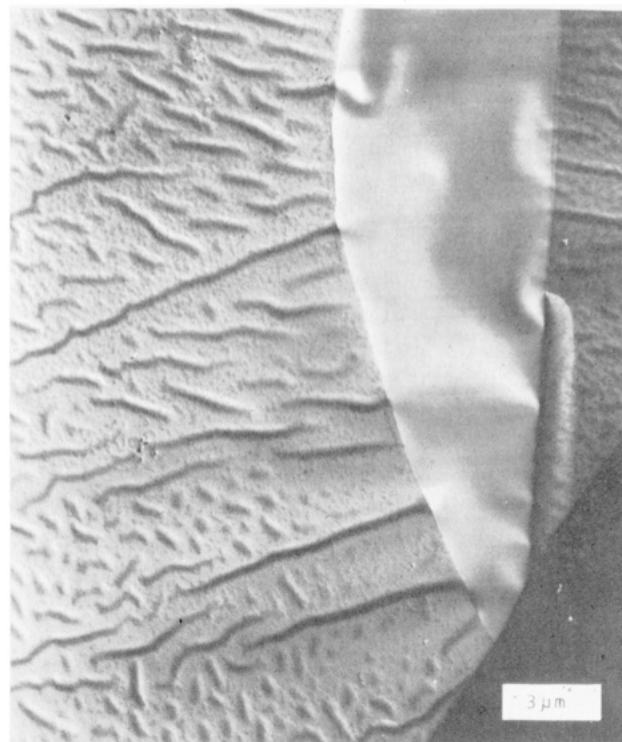


Figure 4. Shadowed replica of thin film of main-chain/side-group liquid crystal polymer.



Figure 5. Electron diffraction pattern of main-chain/side-group liquid crystal polymer showing sharp small-angle reflections and oriented splitted wide-angle halo.

This is clear from the shadowing effect. This surface ripple originates during flow, and its frequency depends on the film thickness. The distance between these thick stripes is in the micrometer range.

Electron Diffraction. For an understanding of the structures observed by dark-field electron microscopy, it is informative to discuss the electron diffraction patterns first. A number of different features are observed. There is a small-angle diffraction maximum with one higher order (indicating a highly oriented system), plus an oriented amorphous halo in the wide-angle region perpendicular to

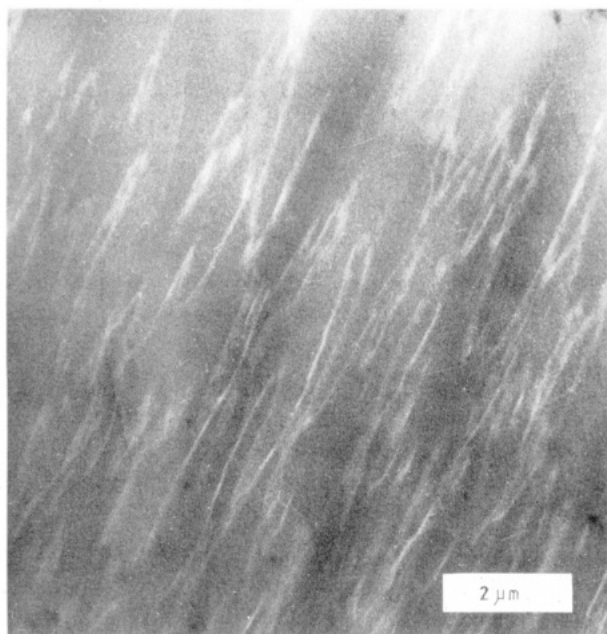


Figure 6. Dark-field micrograph from main-chain/side-group liquid crystal polymer.

it (Figure 5). Such diffraction patterns are typical of smectic liquid crystals with the mesogens in the plane of the film. The measured small-angle spacings are

$$L_1 = 26 \text{ \AA} \quad L_2 = 13 \text{ \AA}$$

The wide angle halo is evaluated by using

$$K\lambda = 2d_a \sin \theta_m$$

The spacing corresponding to this broad maximum is determined by the appropriate Bessel function, the choice of which depends on details of molecular geometry.^{5,6} For smectics, the value of K has been taken to be 1.117, on the basis of the assumption of disordered packing of the molecules. However, if a certain amount of short-range order is assumed, $K = 1.1457$. Therefore, the average intermolecular spacing is either 5.11 or 5.05 Å. Closer inspection reveals that the amorphous halo is, in fact, split (Figure 5) and sharper than is generally observed in amorphous samples.

Dark-Field Electron Microscopy. Dark-field electron microscopy was applied to obtain information about the distribution of the oriented regions giving rise to the small-angle maxima. In this case, an aperture is placed over the diffraction pattern in the focal plane of the objective lens such that only the electrons scattered into the small-angle diffraction maxima are transmitted. These electrons are then used to produce an image (Figure 6). Only those regions that gave rise to the small-angle diffraction maximum now appear bright. It is clear that the oriented areas form quasiparallel regions, a few hundred angstroms thick and several tens of micrometers long. These bright regions obtained by dark-field microscopy deliver true structural information and are totally unrelated to the dark stripes observed in bright-field microscopy, which were shown to arise from thickness undulations, both here and in previous work.⁴

Correlation of these bright, oriented areas with the diffraction pattern shows that the smectic planes are perpendicular to their long direction. Their direction is completely independent of the thick stripes observed in bright-field microscopy. The density of these oriented regions depends on the annealing time, becoming wider and more closely spaced with increasing annealing time.

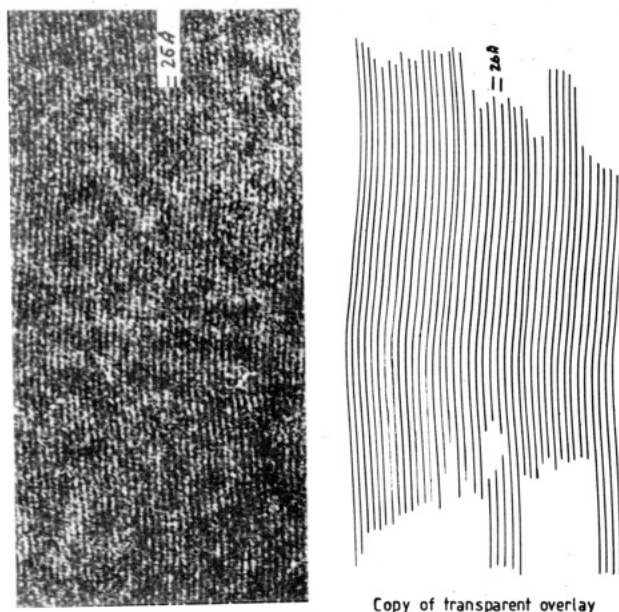


Figure 7. High-resolution electron micrograph of main-chain/side-group liquid crystal polymer and copy of transparent overlay showing undulating smectic planes.

High-Resolution Electron Microscopy. Use is made of the phase-contrast transfer function to obtain contrast variations, enabling lattice planes to be imaged. Phase contrast is produced by the interference of the scattered electron wave that passes through the aperture with the unscattered or background electron wave. We have described the technique and the particular problems involved with these beam sensitive samples previously⁷ and have established that a rather large defocus value must be used to image planes that have a spacing corresponding to typical smectic layer spacings. Furthermore, it is necessary to establish that the films are thin enough to justify neglect of dynamical scattering effects. This is the case if the sample thickness does not exceed $\xi_g/2$, where ξ_g is the extinction distance. An estimation from use of a standard computer program for calculating structure factors indicates that the extinction distance for these liquid crystal polymers in the appropriate direction is about 1800 Å, which is well above twice the film thickness as calculated from the replicas.

The high-resolution images are images of the lattice planes in the bright regions observed in dark-field microscopy at a much higher magnification. Figure 7 shows that the *smectic planes undulate*. This is very clear in the copy of the transparent overlay.

Figure 8 shows an early stage in the development of the smectic planes. They are perpendicular to the direction in which extensive orientation is observed, as had already been predicted from dark-field electron microscopy and electron diffraction. Their spacing is 26 Å, showing that these planes give rise to the small-angle diffraction maximum.

A further series of experiments was performed to determine the dependence of orientation on annealing time. These experiments showed that the oriented regions become broader with increasing annealing time (Figure 9) and finally touch each other until they cover the total area (Figure 10).

Discussion

Since the spacing of the smectic planes (26 Å) corresponds approximately to the length of the side group (24 Å) but not to the distance between mesogenic groups on

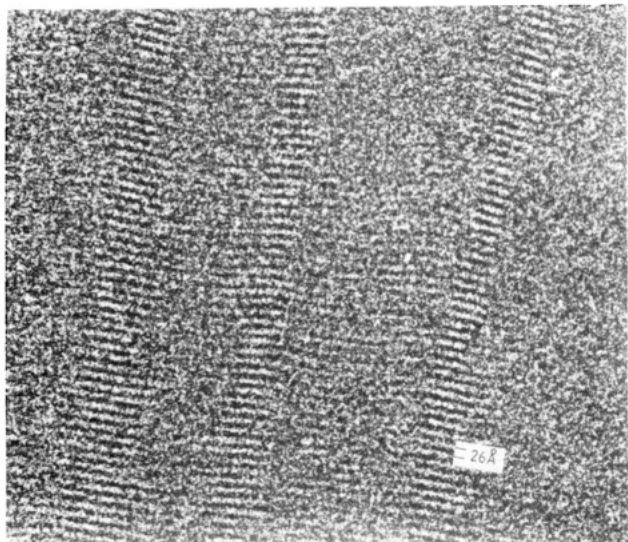


Figure 8. High-resolution electron micrograph of main-chain/side-group polymalonate showing early stages in the development of smectic planes.

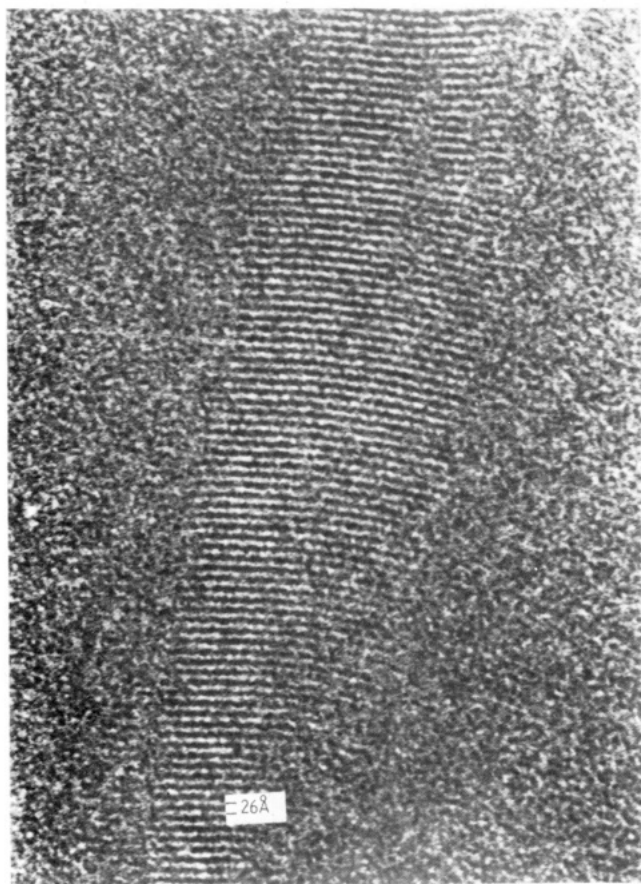


Figure 9. High-resolution electron micrograph showing an intermediate stage in development of smectic planes in main-chain/side-group polymalonate.

the main chain, it is tempting to regard the side groups as being responsible for the formation of the smectic layers in the manner described previously for a pure side-group liquid crystal polymer⁴ with a stiff main chain. This would correspond to model a of Figure 11. Such a structure seems highly improbable since the large volume fraction of disordered main-chain spacer and mesogen would strongly disturb the smectic packing of the side groups. The conformation in Figure 11b is an alternative possibility that seems more probable. In this case, however, the



Figure 10. High-resolution electron micrograph showing final stages in development of undulating smectic planes in main-chain/side-group liquid crystal polymer.

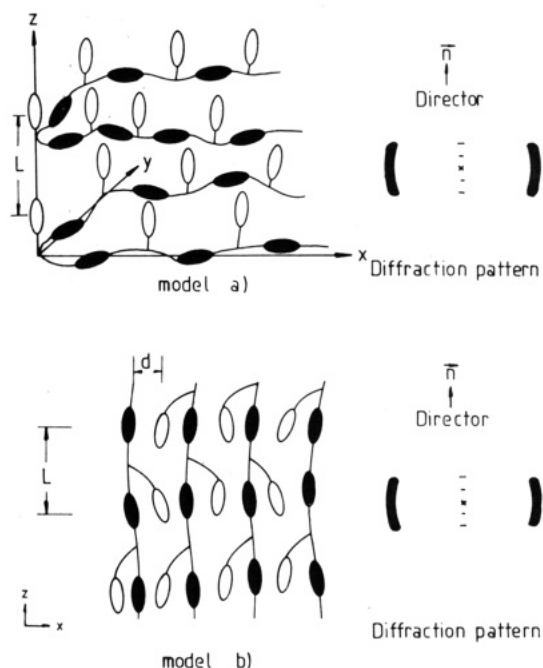
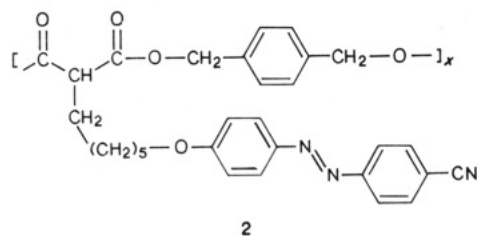


Figure 11. Schematic model and appropriate diffraction pattern for two possible chain conformations giving rise to the observed diffraction pattern.

small-angle spacing of 26 Å is less than the distance between mesogenic groups.

Two further polymers were investigated to determine the contribution of the different structural elements in the main-chain/side-group polymer to the smectic ordering:

(a) A liquid crystal polymalonate with a mesogenic group identical with that in the previous samples but no mesogen in the main chain¹ (2, where the phase transitions (°C) are

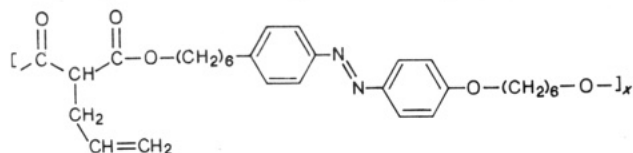


g 35 s 189 i). In this case a smectic phase gave rise to two small-angle maxima (Figure 12) and an oriented wide-angle diffuse halo perpendicular to them (not visible in this diffractogram because this would overexpose the small-angle reflections). The spacings are

$$L_1 = 38.4 \text{ \AA} \quad L_2 = 19.2 \text{ \AA}$$

These values are consistent with the X-ray data obtained for the same polymer.⁸ In view of the large difference between these spacings and those deduced for our main-chain/side-group polymalonate, this experiment indicates that in the side-group polymer the origin of the smectic planes is entirely different from that of the combined main-chain/side-group polymer. Clearly in this case a double layer with intercalation is formed in a manner similar to that proposed previously on the basis of our electron microscopic study of another side-group system.^{4,7}

(b) A liquid crystalline polymer having the identical main chain repeating unit as polymer 1 but no mesogenic side groups⁹ (2, where the phase transitions (°C) are k 34



s_A 132 i). In this case the smectic phase cannot be retained by quenching, and a crystalline phase is formed at room temperature. A highly oriented diffraction pattern is obtained (Figure 13). The small-angle maximum with two higher orders corresponds to a layer spacing

$$L_1 = 36 \text{ \AA}$$

which is almost equal to the spacing between mesogenic groups along the fully extended main chain. This diffraction pattern gives *d* spacings on the equator of 3.8, 3.7, and 3.0 Å.

The finding, therefore, that the smectic layer spacing in main-chain/side-group polymalonate does not correspond to the spacings of the pure main-chain system indicates that while the molecular chain is fully extended in the oriented crystalline main-chain system, it is forced to bend in the liquid crystal main-chain/side-group polymer. That this change is produced by the addition of the side chain to the main chain is not surprising. There are two alternative models that can account for the observed diffraction effects, whereby a combination of both may well represent the true situation:

(a) Since the extended chain length between repeating units is 35 Å, it is necessary to explain the reduction of this length to the observed smectic layer spacing of 26 Å. The model of Figure 1 shows that good chain packing is impossible unless the main chain bends as indicated in Figure 14. The model shows that under these conditions it is possible to pack the shorter side chains such that the mesogenic groups are stacked above one another. It is also possible to understand why the intermolecular oriented halo in the diffraction pattern is split. This is indicated in Figure 14. The observed angle is 33°. A possible model



Figure 12. Diffraction pattern obtained from corresponding pure side-chain liquid crystal polymer.



Figure 13. Diffraction pattern obtained from corresponding pure main-chain liquid crystal polymer.

such as that of Figure 14 requires a reduction of 4 Å in the spacer length from the fully extended conformation. A similar reduction has been observed previously in a side-chain system.⁴ The diffraction evidence (relatively narrow halo and occasional appearance of single-crystal diffraction pattern) indicates that the degree of order is greater than that of a smectic A system. The tilt of the mesogenic group with respect to the director as indicated in Figure 14 would

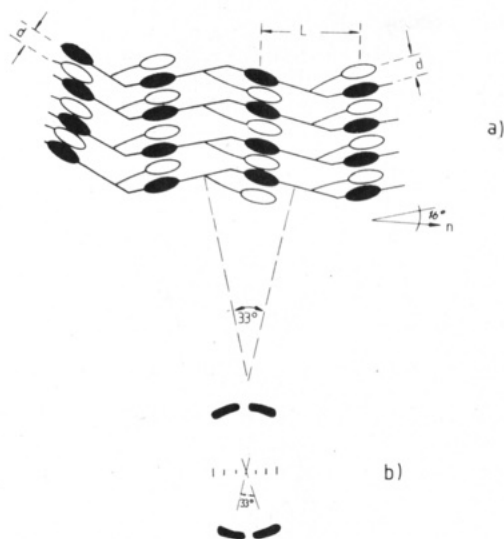


Figure 14. Schematic representation of smectic planes in main-chain/side-group liquid crystal polymalonate (top) with the appropriate diffraction pattern (bottom).

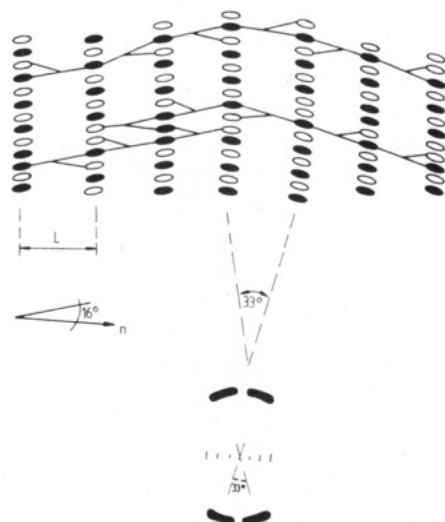


Figure 15. Schematic diagram showing an alternative model of arrangement of smectic planes in liquid crystal main-chain/side-group polymalonate.

suggest a smectic H or G phase.

(b) An alternative version of this basic concept involves larger sequences of the main chain in a particular orientation. The bend between sequences is still 33° to account for the split halo. This model is shown in Figure 15 again, with the required reduction in spacer length. For the sake of clarity, only two of the chains are shown fully connected. In one of these, hairpin bends of the main chain are included to show that such molecular defects may not necessarily disrupt the smectic planes.

We have established, therefore, that the mesogenic group is tilted with respect to the director and that the small-angle maxima are caused by the periodicity of the mesogenic groups along the main chain, whereby the side chains orient parallel to the main chain. This periodicity L is then perpendicular to the main chain, whereby the main chain can, of course, move into the third plane perpendicular to the film. In addition to the bent trajectory of the main chain, the *smectic planes undulate*.

The high-resolution electron micrographs indicate that these smectic planes are *curved*; in fact, they undulate (Figure 7; wavelength $\lambda = 0.1 \mu\text{m}$, amplitude $a = 26 \text{ \AA}$). We have reported such undulations previously for a very

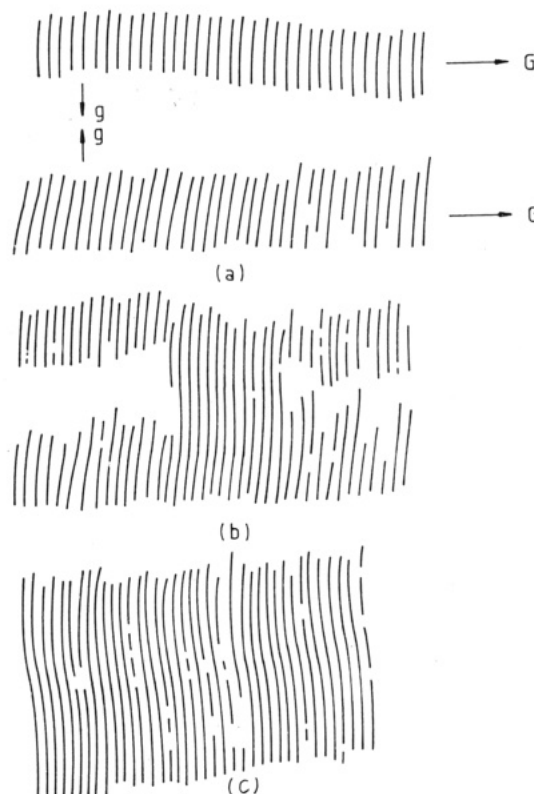


Figure 16. Copy of transparent overlays from high-resolution electron micrographs of main-chain/side-group polymalonate showing development of undulating smectic planes.

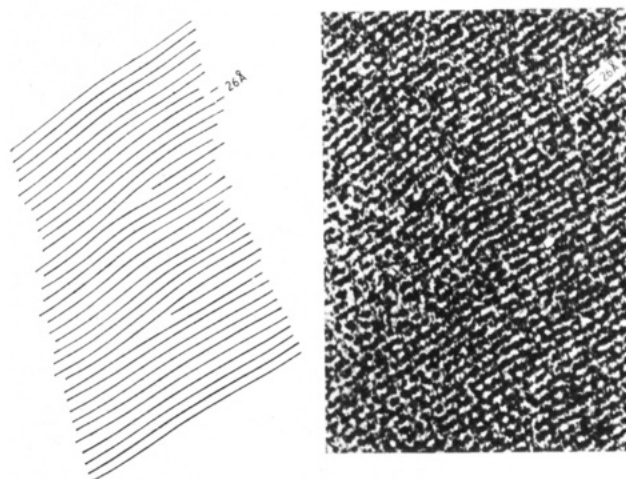


Figure 17. High-resolution electron micrograph showing edge dislocation defects in smectic planes of main-chain/side-group liquid crystal polymalonate.

stiff side-group liquid crystal polymer.^{7,10}

Order in these smectic layers improves with annealing time. Initially very thin oriented regions are observed that have a fast growth direction G perpendicular to the smectic layers. This is indicated schematically in Figure 16a. Subsequently, ordering proceeds in a slow growth direction g perpendicular to G (Figure 16b). Finally, the oriented regions merge (Figure 16c). Sometimes defects arise during this merging operation (Figure 17). The defect that we have chosen for this article represents a simple dislocation. However, many complex situations are observed, which will be published in a subsequent article.¹¹

We have demonstrated in this article the relationship between the molecular chain and the smectic layers in a main-chain/side-group liquid crystal polymer. It has been

shown by dark-field electron microscopy how the oriented regions are distributed in the sample and how these regions grow. With high-resolution techniques, it has been demonstrated that the smectic layers undulate with a characteristic wavelength and amplitude. The nature of defects that arises during the orientation of the sample has been indicated.

Acknowledgment. We are glad to acknowledge our colleagues, particularly Dr. H. Noether and Dr. G. Schmidt, for many stimulating discussions. To the Deutsche Forschungsgemeinschaft we owe special thanks for financial support within the framework of SFB 262.

Registry No. 1 (copolymer), 97104-71-7; 1 (SRU), 97088-50-1.

References and Notes

- (1) Reck, B.; Ringsdorf, H. *Makromol. Chem., Rapid Commun.* **1985**, *6*, 291.
- (2) Reck, B.; Ringsdorf, H. *Makromol. Chem., Rapid Commun.* **1986**, *7*, 389.
- (3) Demus, D.; Richter, L. *Textures of Liquid Crystals*; Verlag Chemie: Weinheim, 1978.
- (4) Voigt-Martin, I. G.; Durst, H. *Liq. Cryst.* **1987**, *2*, 585.
- (5) de Vries, A. *Mol. Cryst. Liq. Cryst.* **1970**, *10*, 219.
- (6) de Vries, A. *Mol. Cryst. Liq. Cryst.* **1985**, *131*, 125.
- (7) Voigt-Martin, I. G.; Durst, H. *Liq. Cryst.* **1987**, *2*, 601.
- (8) Eich, M.; Wendorff, J. H.; Reck, B.; Ringsdorf, H. *Proc. SPIE-Int. Soc. Opt. Eng.* **1986**, *682*, 93.
- (9) Zentel, R.; Schmidt, G. F.; Meyer, J.; Benalia, M. *Liq. Cryst.*, in press.
- (10) Durst, H.; Voigt-Martin, I. G. *Makromol. Chem., Rapid Commun.* **1986**, *7*, 785.
- (11) Voigt-Martin, I. G.; Durst, H., manuscript in preparation.

Highly Ordered Main Chain in a Liquid Crystalline Side-Group Polymer

C. Boeffel and H. W. Spiess*

MPI für Polymerforschung, Postfach 3148, D-6500 Mainz, FRG.

Received September 28, 1987

ABSTRACT: The molecular order of the polymer chain in a liquid crystalline side-group polymer was studied by solid-state ^2H NMR in the frozen smectic phase. In this system the chain is highly extended perpendicular to the mesogens. The NMR data show that the link between the polymer chain and the mesogens is provided by the conformationally ordered quaternary carbon in the polymer chain. The width of the orientational distribution of the C-CH₃ bonds with respect to the director was determined to be $\pm 20^\circ$. The ^2H NMR results are in good agreement with small-angle neutron-scattering studies on the same system.

Introduction

In the spacer model^{1,2} of polymeric side-group liquid crystals the polymer chain is supposed to retain its random coil conformation. Strictly speaking, this requires the absence of any orientation-dependent inter- and intramolecular interactions between the mesogenic group and the polymer chain. Studies on solutions of linear polymers in a liquid crystalline matrix have indeed shown³ that the intermolecular contribution to the orientation effect is small; on the other hand, the mesogenic groups have an ordering effect on the polymer chain through intramolecular forces. The anisotropy of the radii of gyration of the polymer chain in liquid crystalline side-group polymers measured by small-angle neutron scattering (SANS)^{4,5} showed a strong dependence on the mesophase structure of the systems studied. The first ^2H NMR studies on a polyacrylate and a polymethacrylate have shown a different orientation behavior for these two systems with a polymer chain macroscopically oriented parallel and perpendicular to the mesogenic group, respectively.⁶

In this article, ^2H NMR is used to study the local conformation as well as the molecular order of the polymer chain in a polymethacrylate with a high anisotropy of the radii of gyration,⁵ as studied by SANS. A comparison can now be made between the results presented here obtained for systems with the same mesophase structure but with chains of different stiffness and, on the other hand, for systems with different mesophase structures but with chains of the same stiffness.

The mesogenic side group is derived from 4'-butoxyphenyl 4-hydroxybenzoate linked to the polymethacrylate chain via a spacer of six methylene units. ^2H NMR is used as a tool to study the orientation behavior of the polymer chain, which was selectively deuterated. The spectra are

governed by the interaction of the nuclear quadrupole moment with the electric-field gradient of the C- ^2H bond, which is intramolecular in nature. Because of the anisotropy of this interaction the information on the local conformation as well as the orientational distribution of the C- ^2H bonds can be extracted from the spectra in the glassy state. This supplements the findings of the SANS study, from which only the overall coil dimension could be determined.

Experimental Section

The samples were synthesized as described by Ringsdorf et al.⁷ by using deuterated methacrylic acid. The methacrylic acid was prepared from deuterioacetone and HCN. This synthesis was performed by two companies: Roehm at Darmstadt and BASF at Ludwigshafen.

The polymer was characterized by gel permeation chromatography (GPC), calibrated by similar samples of known molecular weight. The number-averaged molecular weight was found to be 60 000, and the polydispersity was 2.3. The phase behavior was characterized by polarization microscopy and by differential scanning calorimetry (DSC). The glass transition was found at 313 K, the transition from the smectic-A to the nematic phase at 381 K, and the clearing temperature at 386 K. The thickness of the smectic monolayers was found by X-ray diffraction to be 2.8 nm.

The ^2H NMR spectra were recorded on a Bruker CXP-300 spectrometer with a home-built probe fitted with a goniometer and obtained by the solid echo technique with quadrature phase detection, as described elsewhere.^{8,9} The sample was macroscopically aligned by the 7-T magnetic field of the NMR spectrometer. To ensure alignment, we heated the sample into the isotropic phase, then tempered it for 1 h at a temperature just below the nematic-isotropic phase transition, and subsequently cooled it slowly below the glass transition temperature over a period of several hours. The angular-dependent measurements were all performed on the glassy state.